The inverse and direct Hofmeister series for lysozyme

Yanjie Zhang and Paul S. Cremer[1]

Department of Chemistry, Texas A&M University, College Station, TX 77843

Communicated by Gabor A. Somorjai, University of California, Berkeley, CA, July 15, 2009 (received for review June 2, 2009)

Anion effects on the cloud-point temperature for the liquid−liquid phase transition of lysozyme were investigated by temperature gradient microfluidics under a dark field microscope. It was found that protein aggregation in salt solutions followed 2 distinct Hofmeister series depending on salt concentration. Namely, under low salt conditions the association of anions with the positively charged lysozyme surface dominated the process and the phase transition temperature followed an inverse Hofmeister series. This inverse series could be directly correlated to the size and hydration thermodynamics of the anions. At higher salt concentrations, the liquid–liquid phase transition displayed a direct Hofmeister series that correlated with the polarizability of the anions. A simple model was derived to take both charge screening and surface tension effects into account at the protein/water interface. Fitting the thermodynamic data to this model equation demonstrated its validity in both the high and low salt regimes. These results suggest that in general positively charged macromolecular systems should show inverse Hofmeister behavior only at relatively low salt concentrations, but revert to a direct Hofmeister series as the salt concentration is increased.

liquid–liquid phase transition | protein aggregation

Protein–protein interactions can lead to aggregation. Such intermolecular contacts underlie the mechanistic basis for a variety of diseases (1–4) and are key to protein crystallization (5–7). An effective way to determine the strength of biomacromolecular interactions is to study the temperature-induced phase separation that occurs in concentrated protein solutions (8). When a concentrated protein solution is cooled below its cloud-point temperature, the system can separate into 2 coexisting liquid phases: 1 rich in protein and 1 poor. As coacervate droplets of the protein-rich phase grow, the solution turns cloudy (white) as a result of the scattering of visible light. Upon standing, the solution may completely separate by gravity into a protein-rich phase and a nearly pure aqueous phase above it. The temperature at which the initial cloud point occurs provides a simple physical measurement of the forces acting among biomacromolecules. Specifically, the higher the temperature at which the initial cloud point occurs, the stronger the putative attractive forces between the protein molecules should be.

Dissolved salts in aqueous solutions have a strong influence on protein–protein interactions and the subsequent aggregated states which are formed. In fact, cloud-point temperatures typically follow a specific ion order according to the Hofmeister series (5, 6, 9–14). The relative effectiveness of anions to induce protein aggregation typically follows 1 of 2 trends depending on the pH of the solution (15, 16). Above a protein's isoelectric point, the macromolecule bears a net negative charge and a direct Hofmeister series is normally observed. In this case, chaotropes such as I^-, ClO_4^-, and SCN^- help to unfold proteins and salt them into solution. By contrast, kosmotropes such as SO_4^{2-} and F^- lead to the stabilization of the folded state and cause a salting-out effect. If the solution pH is below the pI of the protein, the macromolecules are net positively charged. In that case, it has been widely reported that an inverse Hofmeister series is observed (15, 16). Namely, chaotropic anions become more effective at salting-out proteins from solution than kosmotropic anions.

Perhaps the quintessential example of an inverse Hofmeister series is the precipitation of lysozyme from solution (8, 17–24). Herein, we show that lysozyme actually displays an inverse Hofmeister series only at low salt concentration when studied at pH 9.4. As the concentration of monovalent salts is raised, the order reverts back to a direct Hofmeister series. Indeed, the charge screening effects that lead to the inverse series are only dominant below ≈200 or 300 mM salt. Above this concentration, the physical properties follow a direct series. Moreover, we build a simple model based on charge screening and surface tension effects, which can completely account for the hydrophobic collapse and aggregation behavior of these charged macromolecules in the presence of chaotropic anions.

Results and Discussion

Cloud-Point Temperature of Lysozyme vs. Salt Concentration. Fig. 1*A* shows a dark field micrograph from a 6-channel temperature gradient microfluidic assay. The temperature rises linearly across the image from left to right. Dark areas denote regions where proteins are soluble in bulk solution while the purple regions arise from light scattering caused by protein aggregation. The 4 channels in the middle each contain a 90.4 mg/mL lysozyme solution made with 20 mM Tris(hydroxymethyl) aminomethane buffer at pH 9.4. In addition, each solution in channels 2 through 5 contains a different concentration of NaSCN ranging from 0.10 to 0.16 M, respectively. Two polymer solutions with known lower critical solution temperatures (LCSTs) were used as standards to calibrate the temperature gradient (25–30). These channels were placed at the very top and very bottom. At temperatures below the cloud point, the lysozyme solutions were cloudy and scattered light. Above the phase transition temperature, the solutions became clear. By contrast, the polymer solutions at the top and bottom show the opposite behavior. Namely, they are clear at low temperature, but scatter light at higher temperature upon going through their LCST. Fig. 1*B* displays a linescan from the 90.4 mg/mL lysozyme solution with 0.10 M NaSCN. As can be seen, the phase transition occurred over ≈2 °C. The temperature at which the phase transition was completed was used in all data analysis as the cloud-point temperature and is demarked with a vertical red line in the image. This temperature is ≈30.2 °C for the case shown.

Cloud-point temperature measurements were taken at pH 9.4 for 90.4 mg/mL lysozyme solutions as a function of anion type and concentration. These phase transition temperature data are plotted in Fig. 2 for 6 different chaotropic sodium salts. The specific pH and concentration conditions were chosen as they allowed phase transition measurements to be made over a wide range of salt concentrations (see *SI*). The cloud-point behavior is complex and shows different dependencies on anion identity in the low and high salt concentration regions. For all salts except NaCl, the cloud-point temperature increases with salt concen-

Author contributions: Y.Z. and P.S.C. designed research; Y.Z. performed research; Y.Z. and P.S.C. analyzed data; and Y.Z. and P.S.C. wrote the paper.

The authors declare no conflict of interest.

[1]To whom correspondence should be addressed. E-mail: cremer@mail.chem.tamu.edu.

This article contains supporting information online at www.pnas.org/cgi/content/full/0907616106/DCSupplemental.

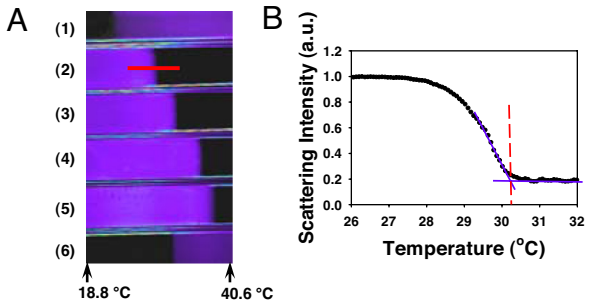

Fig. 1. (*A*) A dark field image from a linear array of 6 microcapillary tubes. Channels 1 and 6 were filled with polymer solutions and used as standards to calibrate the temperature gradient. Channels 2 through 5 were filled with 90.4 mg/mL lysozyme solutions at pH 9.4 with 0.10, 0.12, 0.14, and 0.16 M NaSCN, respectively. (*B*) A light scattering intensity curve taken from the lysozyme solution containing 0.10 M NaSCN. The cloud-point temperature was determined by drawing straight purple lines through the data during the transition and above the transition. The intersection of these lines is denoted by a dashed red vertical line, which is taken to be the cloud-point temperature. The region of the fluorescence micrograph that was used to obtain this linescan is denoted with a red line in *A*.

tration to a maximum value and then decreases linearly. In the low salt regime, the relative effectiveness of the anions follows an inverse Hofmeister series: $ClO_4^- > SCN^- > I^- > NO_3^- > Br^- > Cl^-$. At higher salt concentration, the order reverts to a direct Hofmeister series: $Cl^- > NO_3^- > Br^- > ClO_4^- > I^- > SCN^-$.

Modeling the Phase Transition Data. Despite the apparent complexity of Fig. 2, the aggregation behavior as a function of salt concentration can be explained by the simultaneous occurrence of 2 processes: (*i*) the attenuation of electrostatic repulsion through the specific association of chaotropic anions and (*ii*) the ability of the ions to alter the surface tension of the protein/aqueous interface. Qualitatively, the interplay of these 2 phenomena can be described as follows: Lysozyme is a basic protein with a pI of 11.2 (15) and, hence, its surface is positively charged at pH 9.4. Repulsive electrostatic interactions between lysozyme molecules keep them from flocculating at low salt concentrations. The presence of electrolyte ions in the solution, however, changes this situation. When chaotropic anions associate with positively charged sites on the protein surface, the effective surface charge on the macromolecule will be reduced (31–33). This in turn diminishes the surface potential of the protein/water interface causing the cloud-point temperature to rise. On the other hand, ions partitioning to the protein/water interface will also modulate the interfacial tension (34). For example, if the surface tension is increased, this will cause protein aggregation and thereby increase the cloud-point temperature.

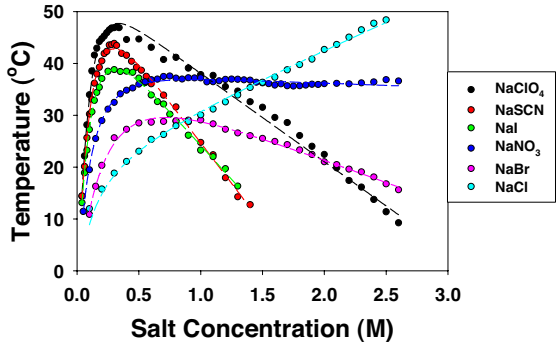

Fig. 2. The cloud-point temperature of lysozyme as a function of anion type and concentration. All experiments were conducted with 90.4 mg/mL lysozyme in 20 mM Tris buffer at pH 9.4. The dashed lines are fits to the data points using Eq. **1**.

To a first approximation, the specific association behavior of chaotropic anions can be modeled by a Langmuir-type isotherm (25–27, 35). However, because electrostatic neutralization is involved, an exponential factor must be added (36) and the justification for this is provided in the *SI*. By contrast, the surface tension should simply vary linearly with salt concentration (25–27, 34, 37–39). Therefore, the data in Fig. 2 can be modeled by Eq. **1**, which includes a constant, a modified binding isotherm, and a linear term:

$$T = T_0 + \frac{B_{\max}[M]e^{-b[M]}}{K_d + [M]e^{-b[M]}} + c[M] \qquad [1]$$

Here, T_0 is the cloud-point temperature of lysozyme in the absence of salt, and $[M]$ is the molar concentration of salt. The constant, $B_{\max}$, has units of temperature and represents the maximum increase in cloud-point temperature when all of the positive charges on protein surface have anions associated with them. The constant, b, has units of reciprocal molarity and is an electrostatic interaction factor that is related to the surface potential of lysozyme. The values of both $B_{\max}$ and b are measures of the effectiveness for a specific anion to associate with positive charges on the protein surface and thereby attenuate the electrostatic repulsion between the charged macromolecules. By contrast, the constant, c, has units of temperature/molarity and characterizes specific anion effects on the interfacial tension at the protein/water interface. The dashed lines in Fig. 2 are fits to the data with Eq. **1**. The abstracted values for K_d, $B_{\max}$, b, and c are provided in Table 1 along with relevant thermodynamic information for the anions. It should be noted that Eq. **1** is completely general and can also be applied to neutral systems. In that case the exponential term goes to 1 because b goes to 0 (25–27).

To more clearly visualize the inverse and direct Hofmeister effects for lysozyme aggregation, the binding and the interfacial tension contributions to the cloud-point temperature can be plotted separately. This can be done by subtracting the linear fit ($T_0 + c[M]$) to the cloud-point data in Fig. 2 and replotting the residual values as a function of salt concentration (Fig. 3*A*). As can be seen, a saturation type binding curve is revealed. Moreover, subtracting the binding contribution from Fig. 2 and replotting the residuals shows linear behavior as a function of salt concentration (Fig. 3*B*). Strikingly, the binding curve behavior and the linear behavior can be seen to obey an inverse and direct Hofmeister series, respectively. Because the binding curves represent a saturation phenomenon, they cease to show much change after 200 or 300 mM of salt. On the other hand, the linear term associated with the interfacial tension remains effective up to at least several moles of salt.

Anion Binding and Ionic Volume. Changes in the aqueous solution volume upon addition of salt provides vital information on the hydration of inorganic anions by adjacent water molecules (40). Both the $B_{\max}$ and b values abstracted from fits to the data in Fig. 2 are well correlated with the partial molar volumes (V_i^0) of the anions (Fig. 4*A* and *B*). Partial molar volume values for ions have previously been interpreted to describes the size of the hydrated ions (41). As can be seen from the data, the larger anions are more effective at associating with the positively charged lysozyme surface. As a consequence, these anions are more efficient at screening the electrostatic repulsion between protein molecules and promoting salting-out behavior. Therefore, an inverse Hofmeister series is followed according to the hydrated volume of the anions. Such a finding is consistent with previous

Table 1. Fitted values for K_d, B_{max}, b, and c from cloud-point temperature measurements and literature values for some thermodynamic properties

Anion	V_i^0 (cm³/mol)	ΔG_{hydr} (KJ/mol)	α (10^{-30} m³)	$\sigma_{air/water}$ (mN L/mM)	K_d (M)	B_{max} (°C)	b (M^{-1})	c (°C/mol)	$\sigma_{lysozyme/water}$ (mN L/mM)
ClO_{4-}	49.6	−214	5.062	1.4	0.10	60.1	−7.02	−17.0	−2.7
SCN−	41.2	−287	6.739	0.5	0.10	61.1	−5.35	−31.4	−5.0
I−	41.7	−283	7.512	1.0	0.09	55.5	−4.89	−26.3	−4.2
NO_{3-}	34.5	−306	4.134	1.1	0.10	42.9	−3.21	−0.9	−0.1
Br−	30.2	−321	4.852	1.3	0.18	43.8	−1.75	−8.7	−1.4
Cl−	23.3	−347	3.421	1.6	0.12	28.1	−0.10	10.3	1.6

The estimated interfacial tension increments for the anions at the protein/water interface ($\sigma_{protein/water}$) are also listed. V_i^0, ΔG_{hydr}, and α data are from ref. 43; σ data are from ref. 59. Note that 10^{-30} m³ = 1 Å³

observations that the efficacy of different salts for screening charge–charge interactions correlates with the denaturing strength of the ions and consequently the position of the ions in the Hofmeister series (42).

The partial molar volume V_i^0 for a given anion in aqueous solution is directly proportional to its hydration free energy, ΔG_{hydr} (43). Moreover, the free energy of ion hydration is typically defined as its transfer from a fixed point in vacuum to a fixed point in the solution (44). The direct correlation between V_i^0 and ΔG_{hydr} necessarily implies that B_{max} and b are also linearly correlated to ΔG_{hydr} (see *SI*). This leads to a simple mechanistic picture for the inverse Hofmeister series of lysozyme. Namely, bigger anions have a lower free energy cost for shedding their hydration shells and engaging in ion pairing relative to smaller anions. It should also be noted that bigger anions also have fewer water molecules in their hydration shells (45). X-ray crystallography has revealed the presence of associated anions in lysozyme crystals when they are grown in the presence of the corresponding salt solution (46, 47). The anions are not randomly distributed on protein surface, but instead prefer to interact with specific hydrophilic residues, especially those which are positive charged such as Arg and Lys (46, 47). The distance between individual anions and the protein binding sites in the crystal structures indicate that intervening water is not present, although water molecules may be directly involved in anion–lysozyme interactions in solution.

Interfacial Tension and Polarizability. As a lysozyme solution is lowered below its cloud-point temperature, the formation of coacervate droplets rapidly reduces the area of the protein/bulk water interface. Moreover, the partitioning of anions to this interface modulates the interfacial tension and thereby the thermodynamics of protein aggregation (34, 48). It is well known that interfacial tension for the air/water and many hydrocarbon/water interfaces varies linearly with salt concentration up to at least moderate ionic strengths (37–39). As shown above, subtracting the binding contribution to the cloud-point vs. salt concentration data in Fig. 2, reveals a linear

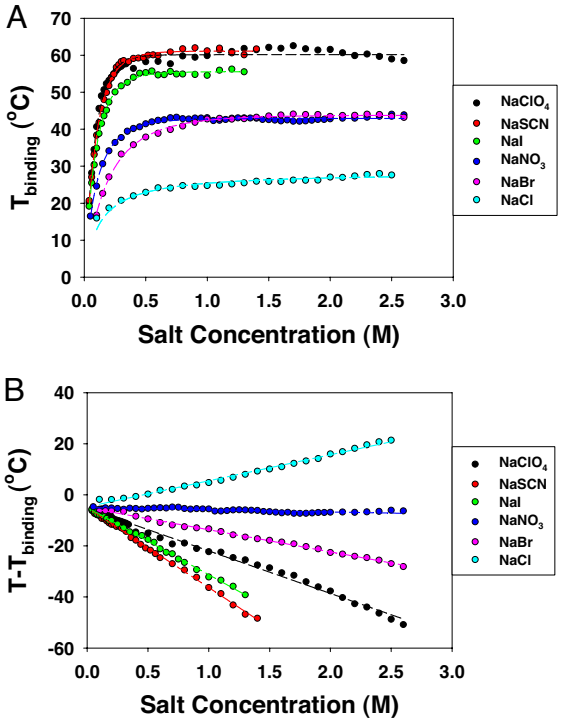

Fig. 3. (*A*) Residual cloud-point temperature data from Fig. 2 after subtracting the linear portion from the curves. (*B*) The residual cloud-point temperature data after removing the binding term. The dashed lines represent fits to the data points.

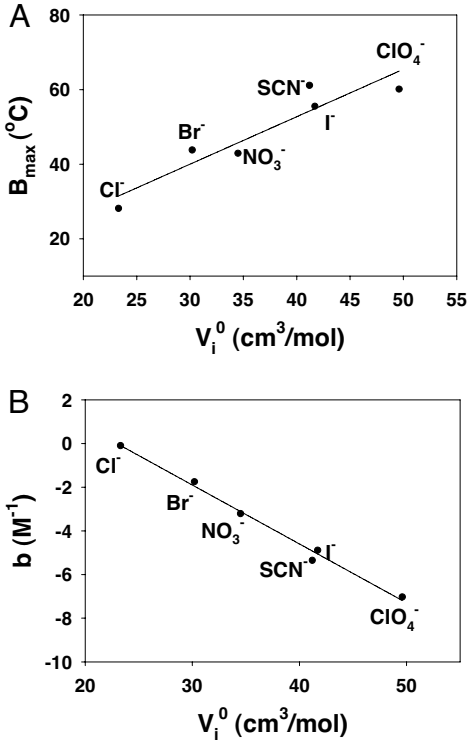

Fig. 4. (*A*) Plot of partial molar volume of the anions vs. B_{max}. (*B*) Plot of the partial molar volumes of anions vs. the constant, b.

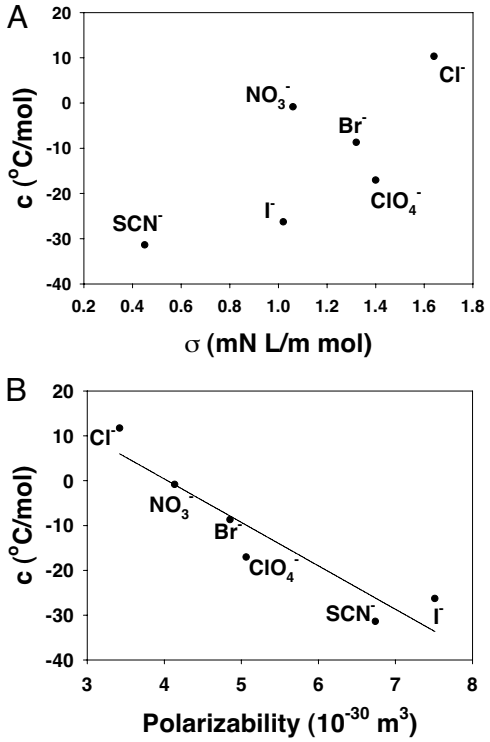

Fig. 5. (*A*) Plot of surface tension increment values for the anions at the air/water interface vs. the constant, *c*. (*B*) Plot of polarizability values for the anions vs. the constant, *c*. Polarizability data are taken from ref. 43.

dependence between the residual cloud-point data and salt concentration (Fig. 3*B*). With the exception of chloride, the slopes of all of these lines are negative, which indicates that increasing the salt concentration actually lowers the interfacial tension and thereby the cloud-point temperature. Such behavior is consistent with the effect of chaotropic ions at aqueous/oil interfaces, where more chaotropic ions such as I^- and SCN^- are known to decrease surface tension, while Cl^- is actually known to increase it (49, 50). Moreover, it has been proposed that the salt-induced change of interfacial tension at protein/water interfaces may be either positive or negative depending on the particular salt (51). By contrast, the sodium salts of all these ions raise the surface tension at the air/water interface (37–39). As such, the slopes of the lines in Fig. 3*B* (*c* values from Eq. **1**) are uncorrelated with the known surface tension increment values of the air/water interface (Fig. 5*A*). Instead, a strong correlation is noted with the polarizability of the ions (Fig. 5*B*).

The polarizability of an anion reflects the ability of its electronic shell to undergo deformation in an electric field. This constant is usually reported in dimensions of volume (43). As can be seen in Fig. 5*B*, the most polarizable anions exhibit the strongest tendency to decrease the interfacial tension at the protein/water interface and salt in the protein. This finding is consistent with the partitioning of compounds in octanol/water systems where the octanol/water partition coefficient has been shown to be directly correlated with the polarizability of a given compound (52, 53). Specifically, more polarizable compounds tend to partition to the oil phase compared to the aqueous phase. This notion is also consistent with molecular dynamics simulations that show that ions with low charge density exhibit preferential binding to hydrophobic surface moieties and to hydrophobic plates in aqueous solution (33, 54).

The results shown in Fig. 5 are quite curious in light of the fact that surface tension data from the air/water interface correlate quite well with changes in the LCST values for poly(*N*-isopropylacrylamide) and elastin-like polypeptides in the presence of chaotropic anions (25–27). Of course, the LCST of those systems involves hydrophobic collapse. In the present case, the lysozyme molecules are already folded and the dielectric constant of the surface should be significantly higher than for hydrophobically hydrated polymer molecules (55–58).

The interfacial tension increments at the lysozyme/water interface for the sodium salts of all of the chaotropic ions used in these studies are abstracted by fitting the linear portion of the data in Fig. 2. This can be done by using Cl^- as the calibrating ion, because it is known that its interfacial tension increment value is approximately the same at the air/water and oil/water interface (50). By extension, we assume this value also remains constant at the protein/water interface. The surface tension increment values are reported in Table 1. To the best of our knowledge, these data represent the first experimentally determined estimates for interfacial tension increments at a protein/water interface.

Generality of the Reversed and Direct Hofmeister Series. The mechanism for the modulation of the liquid–liquid phase transition temperature of lysozyme by specific anions depends on the ionic volume and the polarizability of the anions as shown above. Such a finding is consistent with the idea that the anions partition to the protein/water interface and can directly associate with positively charged surface moieties. The influence of charge pairing is relatively strong and displays saturation behavior after the addition of a few hundred mM of monovalent salts. On the other hand, anion partitioning to the protein/water interface does not display saturation behavior under the conditions that were investigated, but is significantly weaker. As a consequence, the cloud-point temperature behavior for the liquid–liquid phase transition of lysozyme appears to be relatively complex. For more chaotropic anions, the phase transition temperature rises sharply at low concentration because of ion pairing, but then reaches a maximum and reverses because of the decrease in the interfacial tension. The behavior of NaCl is different. The cloud-point temperature rises at low salt concentration because of ion pairing; however, the phase transition temperature continues to rise as the interfacial tension goes up at higher concentration. This type of strong ion pairing and relatively weak surface tension behavior may be general. As a consequence, other positively charged systems that display inverse Hofmeister behavior at low salt concentration may also revert to a direct Hofmeister series as the salt concentration is raised.

Materials and Methods

Hen egg white lysozyme was obtained from Fisher Scientific (catalog no. 61193-0050). It was subjected to dialysis to remove salt and the protein was lyophilized to form a powder. The powdered protein was redissolved in 20 mM Tris(hydroxymethyl) aminomethane buffer in all cases. The inorganic salts used in these experiments were purchased from Aldrich. Low-conductivity H_2O, produced from a NANOpure Ultrapure Water System (Barnstead) with a minimum resistivity of 18 MΩ·cm, was used to prepare the buffer solutions. The protein solutions were prepared at twice the desired final concentration and salt solutions were added immediately before the samples were placed onto the testing platform. All cloud-point measurements were carried out with a linear temperature gradient microfluidic platform inside capillary tubes, which has been described previously (25–30). The measurements had a typical standard error of ±0.1 °C. Experimental conditions other than pH 9.4 and 90.4 mg/mL lysozyme were also explored and are described in the *SI*.

ACKNOWLEDGMENTS. This work was supported by the National Science Foundation (CHE-0809854) and the Robert A. Welch Foundation (A-1421).

1. Benedek GB (1997) Cataract as a protein condensation disease: The proctor lecture. *Invest Ophth Vis Sci* 38:1911–1921.
2. Benedek GB, Pande J, Thurston GM, Clark JI (1999) Theoretical and experimental basis for the inhibition of cataract. *Prog Retin Eye Res* 18:391–402.
3. Dobson CM (2003) Protein folding and misfolding. *Nature* 426:884–890.
4. Gaggelli E, Kozlowski H, Valensin D, Valensin G (2006) Copper homeostasis and neurodegenerative disorders (Alzheimer's, prion, and Parkinson's diseases and amyotrophic lateral sclerosis). *Chem Rev* 106:1995–2044.
5. Curtis RA, Prausnitz JM, Blanch HW (1998) Protein-protein and protein-salt interactions in aqueous protein solutions containing concentrated electrolytes. *Biotechnol Bioeng* 57:11–21.
6. Curtis RA, Ulrich J, Montaser A, Prausnitz JM, Blanch HW (2002) Protein-protein interactions in concentrated electrolyte solutions: Hofmeister-series effects. *Biotechnol Bioeng* 79:367–380.
7. Annunziata O, Payne A, Wang Y (2008) Solubility of lysozyme in the presence of aqueous chloride salts: Common-ion effect and its role on solubility and crystal thermodynamics. *J Am Chem Soc* 130:13347–13352.
8. Broide ML, Tominc TM, Saxowsky MD (1996) Using phase transitions to investigate the effect of salts on protein interactions. *Phys Rev E* 53:6325–6335.
9. Hofmeister F (1888) Zur lehre von der wirkung der salze (Lessons on the effects of salts). *Arch Exp Pathol Pharmakol* 24:247–260.
10. Collins KD (2004) Ions from the Hofmeister series and osmolytes: Effects on proteins in solution and in the crystallization process. *Methods* 34:300–311.
11. Curtis RA, Lue L (2006) A molecular approach to bioseparations: Protein-protein and protein-salt interactions. *Chem Eng Sci* 61:907–923.
12. Kunz W, Lo Nostro P, Ninham BW (2004) The present state of affairs with Hofmeister effects. *Curr Opin Colloid Interface Sci* 9:1–18.
13. Petersen PB, Saykally RJ (2006) On the nature of ions at the liquid water surface. *Annu Rev Phys Chem* 57:333–364.
14. Smith JD, Saykally RJ, Geissler PL (2007) The effect of dissolved halide anions on hydrogen bonding in liquid water. *J Am Chem Soc* 129:13847–13856.
15. Boström M, et al. (2005) Why forces between proteins follow different Hofmeister series for pH above and below pI. *Biophys Chem* 117:217–224.
16. Finet S, Skouri-Panet F, Casselyn M, Bonnete F, Tardieu A (2004) The Hofmeister effect as seen by SAXS in protein solutions. *Curr Opin Colloid Interface Sci* 9:112–116.
17. Wentzel N, Gunton JD (2007) Liquid-liquid coexistence surface for lysozyme: Role of salt type and salt concentration. *J Phys Chem B* 111:1478–1481.
18. Ishimoto C, Tanaka T (1977) Critical behavior of a binary mixture of protein and salt-water. *Phys Rev Lett* 39:474–477.
19. Taratuta VG, Holschbach A, Thurston GM, Blankschtein D, Benedek GB (1990) Liquid-liquid phase separation of aqueous lysozyme solutions: Effects of pH and salt identity. *J Phys Chem* 94:2140–2144.
20. Grigsby JJ, Blanch HW, Prausnitz JM (2001) Cloud-point temperatures for lysozyme in electrolyte solutions: Effect of salt type, salt concentration and pH. *Biophys Chem* 91:231–243.
21. Muschol M, Rosenberger F (1997) Liquid-liquid phase separation in supersaturated lysozyme solutions and associated precipitate formation/crystallization. *J Chem Phys* 107:1953–1962.
22. Riès-Kautt MM, Ducruix AF (1989) Relative effectiveness of various ions on the solubility and crystal-growth of lysozyme. *J Biol Chem* 264:745–748.
23. Riès-Kautt MM, Ducruix AF (1991) Crystallization of basic-proteins by ion-pairing. *J Cryst Growth* 110:20–25.
24. Riès-Kautt MM, Ducruix A (1997) Inferences drawn from physicochemical studies of crystallogenesis and precrystalline state. *Method Enzymol* 276:23–59.
25. Zhang YJ, Furyk S, Bergbreiter DE, Cremer PS (2005) Specific ion effects on the water solubility of macromolecules: PNIPAM and the Hofmeister series. *J Am Chem Soc* 127:14505–14510.
26. Zhang YJ, et al. (2007) Effects of Hofmeister anions on the LCST of PNIPAM as a function of molecular weight. *J Phys Chem C* 111:8916–8924.
27. Cho Y, et al. (2008) Effects of Hofmeister anions on the phase transition temperature of elastin-like polypeptides. *J Phys Chem B* 112:13765–13771.
28. Mao HB, Li CM, Zhang YJ, Bergbreiter DE, Cremer PS (2003) Measuring LCSTs by novel temperature gradient methods: Evidence for intermolecular interactions in mixed polymer solutions. *J Am Chem Soc* 125:2850–2851.
29. Zhang YJ, Mao HB, Cremer PS (2003) Probing the mechanism of aqueous two-phase system formation for α-elastin on-chip. *J Am Chem Soc* 125:15630–15635.
30. Zhang YJ, Trabbic-Carlson K, Albertorio F, Chilkoti A, Cremer PS (2006) Aqueous two-phase system formation kinetics for elastin-like polypeptides of varying chain length. *Biomacromolecules* 7:2192–2199.
31. Lund M, Jungwirth P (2008) Ion specific protein assembly and hydrophobic surface forces. *Phys Rev Lett* 100:258105.
32. Lund M, Vácha R, Jungwirth P (2008) Specific ion binding to macromolecules: Effects of hydrophobicity and ion pairing. *Langmuir* 24:3387–3391.
33. Lund M, Vrbka L, Jungwirth P (2008) Specific ion binding to nonpolar surface patches of proteins. *J Am Chem Soc* 130:11582–11583.
34. Pegram LM, Record MT (2008) Thermodynamic origin of Hofmeister ion effects. *J Phys Chem B* 112:9428–9436.
35. Chen X, Yang T, Kataoka S, Cremer PS (2007) Specific ion effects on interfacial water structure near macromolecules. *J Am Chem Soc* 129:12272–12279.
36. Israelachvili JN (1991) in *Intermolecular and Surface Forces* (Academic, San Diego), pp. 213–259.
37. Jarvis NL, Scheiman MA (1968) Surface potentials of aqueous electrolyte solutions. *J Phys Chem* 72:74–78.
38. Pegram LM, Record MT (2006) Partitioning of atmospherically relevant ions between bulk water and the water/vapor interface. *Proc Natl Acad Sci USA* 103:14278–14281.
39. Pegram LM, Record MT (2007) Hofmeister salt effects on surface tension arise from partitioning of anions and cations between bulk water and the air-water interface. *J Phys Chem B* 111:5411–5417.
40. Akitt JW (1980) Limiting single-ion molar volumes: Intrinsic volume as a function of the solvent parameters. *J Chem Soc Farad Trans I* 76:2259–2284.
41. Marcus Y (1985) *Ion Solvation* (John Wiley and Sons, Malden, MA).
42. Perez-Jimenez R, Godoy-Ruiz R, Ibarra-Molero B, Sanchez-Ruiz JM (2004) The efficiency of different salts to screen charge interactions in proteins: A Hofmeister effect? *Biophys J* 86:2414–2429.
43. Marcus Y (1997) *Ion Properties* (Marcel Dekker, New York, NY).
44. Marcus Y (1987) Thermodynamics of ion hydration and its interpretation in terms of a common model. *Pure Appl Chem* 59:1093–1101.
45. Marcus Y (1991) Thermodynamics of solvation of ions. 5. Gibbs free-energy of hydration at 298.15 K. *J Chem Soc Farad Trans I* 87:2995–2999.
46. Steinrauf LK (1998) Structures of monoclinic lysozyme at 1.6 Å and triclinic lysozyme nitrate at 1.1 Å. *Acta Crystallogr D* 54:767–779.
47. Vaney MC, et al. (2001) Structural effects of monovalent anions on polymorphic lysozyme crystals. *Acta Crystallogr D* 57:929–940.
48. Pegram LM, Record MT (2008) Quantifying accumulation or exclusion of H^+, HO^-, and Hofmeister salt ions near interfaces. *Chem Phys Lett* 467:1–8.
49. Guest WL, Lewis WCM (1939) The effect of electrolytes upon the interfacial tension between water and dekalin (*trans*-decahydronaphthalene). *Proc R Soc Lond A* 170:501–513.
50. Aveyard R, Saleem SM (1976) Interfacial-tensions at alkane-aqueous electrolyte interfaces. *J Chem Soc Farad Trans I* 72:1609–1617.
51. Dér A, et al. (2007) Interfacial water structure controls protein conformation. *J Phys Chem B* 111:5344–5350.
52. Lewis DFV (1989) The calculation of molar polarizabilities by the CNDO/2 method: Correlation with the hydrophobic parameter, logP. *J Comp Chem* 10:145–151.
53. Breindl A, Beck B, Clark T (1997) Prediction of the *n*-octanol/water partition coefficient, logP, using a combination of semiempirical MO-calculations and a neural network. *J Mol Model* 3:142–155.
54. Zangi R, Hagen M, Berne BJ (2007) Effect of ions on the hydrophobic interaction between two plates. *J Am Chem Soc* 129:4678–4686.
55. Schutz CN, Warshel A (2001) What are the dielectric ''constants'' of proteins and how to validate electrostatic models? *Proteins* 44:400–417.
56. Lund M, Jönsson B, Woodward CE (2007) Implications of a high dielectric constant in proteins. *J Chem Phys* 126:225103.
57. Dwyer JJ, et al. (2000) High apparent dielectric constants in the interior of a protein reflect water penetration. *Biophys J* 79:1610–1620.
58. Karp DA, et al. (2007) High apparent dielectric constant inside a protein reflects structural reorganization coupled to the ionization of an internal Asp. *Biophys J* 92:2041–2053.
59. Melander W, Horvath C (1977) Salt effects on hydrophobic interactions in precipitation and chromatography of proteins: Interpretation of lyotropic series. *Arch Biochem Biophys* 183:200–215.